

Research on the working life at steel wire ropes in contact

Vilceanu Lucia, Ghita Eugen, Puțan Vasile

Abstract— In this paper, the authors thought contact pressure wires and the rope take-up roller played an important role in steel ropes' working life and investigate it by using experiments and numerical methods. During the examination of the wires that make up an out of order rope, evidence was found that the request of local compression between wires had such high values that a print appeared on the wire on the contact area. The contact stress appears between the wires of the same rope strand, of two adjacent rope strands and between the wires and the rope take-up roller. The paper shows the research regarding the induced and deforming stress at the moment of contact between wires and the traction cable take-up roller. The results got after running the program, post-processed in strips with equal stress and displacement indicated symmetry of the stress-strain state according with the theory. The results will be used to calculate the fatigue crack propagation and to estimate the steel rope working life.

Keywords— contact pressure, finite element method, numerical analysis, stress-strain state, working life.

I. INTRODUCTION

The wire ropes' durability, equated with the service life of the wire ropes, is determined to some extent by their appropriate choice and their rational exploitation. Using the best types of steel ropes, in different industrial areas, finding better ways for improving their quality and their exploitation conditions, will lead to the increase of their durability, the safety of the exploitation and to the achieving of great savings for the industry. These savings may come from the reduction of the rope consumption, thus from the reduction of quality steel consumption and from the cutting of break times in production, necessary for replacement of used ropes. During operation we encounter a supervised behavior of the ropes because terms for replacing used ropes are always followed and the quality of the wire components is periodically checked. Withdrawing the rope from exploitation [2] is operated when one or more of the following conditions are fulfilled:

- a) ropes reaching their service life, evaluated in tones-kilometers or kilometers- time in connection with the weight per meter of cable.
- b) reaching a certain number of broken wires per cable pace.
- c) the decrease of the safety coefficient of the cable at a certain value, the decrease of the real laceration force of the cable and diminishing of the number of bents until the breaking of the wires settles at the regular control testing. If during one of these current tests 25% of the wire components do not fit the standards, the cable is squashed.

d) if during a macroscopic examination the deterioration of a strand is found, the breaking of the wires on a certain section is accelerating or an accentuated wear is found in one of its areas due to rust and corrosion.

During the examination of the wires that make up an out of order cable, evidence was found that the request of local compression between wires had such high values that a print appeared on the wire on the contact area. Contact requests appear among wires of the same strand, among wires belonging to bordered strands and among wires and the rope take-up roller. The parameters involved in the evaluation of the stress state and wear [1], belonging to wires in contact, may refer to: the geometry of contact elements, the statistic and tribology of the contact, mechanical characteristics of the materials, operating factors. These parameters possess a simultaneously influence during contact, conditioning and influencing each other, which leads to a mingling of the result of their action.

II. PROBLEM FORMULATION

The estimation of the real stresses in the cross-section of the wire rope is very difficult because the wires are placed under different angles reported to the axes. There are subjected not only to traction, but also to bending and torsion. So, the state of stress in the wires is very sophisticated after the wiring manufacturing process. According to the hypothesis which fundament the strength calculus [1], the mechanical loads in the wires of a wire rope are considered as statically loads type Saint-Venant: traction, bending and secondary bending because of the support of a wire to other two adjacent wires, respectively the static contact loading type Hertz or Steuermann.

The classical contact theory between the elastic bodies, which was proposed by Hertz and Beleaev [1], allowed the approximation that the contact surface sizes have very small dimensions in comparison with the dimensions of the bodies in contact. The classical theory did not consider important aspects which lead to difficulties in obtaining the solution. It represents the non-linear aspects of every contact problem, leading to a non-iterative solution.

According to Hertz's theory, the initial contact takes place in a single point, resulting an ideal case which is not often found in practice [4]. The contact between conformal surfaces didn't allow approximating the surface equations by second order polynomial functions, as Hertz considered for the non-conformal surfaces, neglecting the higher order terms.

In order to eliminate the approximations, new theories (Panton, Steuermann and others) have been advanced

during the time in order to calculate the state of stress and deformation in contact problems.

The initial distance h between the points placed on a common vertical line which will be in contact in the next moments is:

$$h = z_1 + z_2 = A_1 x^2 + A_2 x^4 + \dots + A_n x^{2n} + \dots \quad (1)$$

The mathematical relation is valid for the two-dimensional contact when the surfaces in contact present symmetry to the initial contact point. When the bodies in contact present symmetry to an initial contact axis, the following mathematical relation is convenient to be used:

$$h = A_1 r^2 + A_2 r^4 + \dots + A_n r^{2n} + \dots \quad (2)$$

The surfaces in contact z_1 and z_2 which for Hertz approximated their equations, correspond to the case $n = 1$.

For an axis-symmetrical contact [9], Steuermann used sophisticated mathematical relations for pressure and displacement (compression):

$$p_n(r) = \frac{n A_n E^* a^{2n-2}}{\pi} \left[\frac{2 \cdot 4 \dots 2n}{1 \cdot 3 \dots (2n-1)} \right]^2 \left[\left(\frac{r}{a} \right)^{2n-2} + \frac{1}{2} \left(\frac{r}{a} \right)^{2n-4} + \dots + \frac{1 \cdot 3 \dots (2n-3)}{2 \cdot 4 \dots (2n-2)} \right] (a^2 - r^2)^{\frac{1}{2}}$$

Respectively:

$$\delta = \frac{2 \cdot 4 \dots 2n}{1 \cdot 3 \dots (2n-1)} A_n a^{2n} \quad (3)$$

A particular problem, with an important practical application, and which has been analyzed by some authors [1], [2], [4] and [9] is represented by the contact between a cylinder and a cylinder cavity (Fig.1). According to Steuermann's theory, the bodies in contact will not be considered as elastic half-spaces. Moreover the radius difference $\Delta R = R_2 - R_1$ present small values in comparison both with R_1 and R_2 .

In case of a linear contact on the common generatrix between a cylinder and a cylinder cavity with parallel axes (Fig.1) the value of the ratio $q = Q/I$ represents the uniformly distributed pressure on the initial common contact generatrix.

The deformed contact zone is presented in Fig.2. The points belonging to surfaces S_1 and S_2 , which will come in contact on a common surface S , will present both radial u_r , and tangential u_θ displacements.

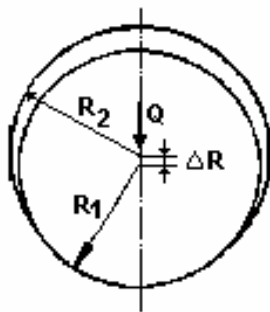


Fig.1. The contact between a circular cylinder and a cylinder cavity

If $\delta \ll R_1, R_2$, the following geometrical relation is valid:

$$(R_2 + \bar{u}_{r2}) - (R_1 + \bar{u}_{r1}) = (\Delta R + \delta) \cos \Phi \quad (4)$$

Resulting: $\bar{u}_{r2} - \bar{u}_{r1} = \delta \cos \Phi - \Delta R(1 - \cos \Phi)$

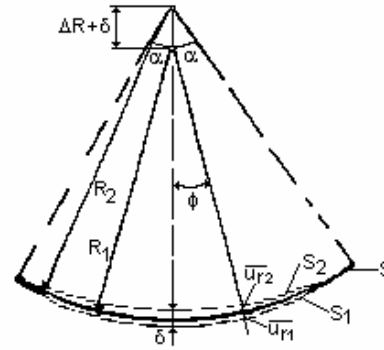


Fig.2. The deformed state in the contact zone

Because $-\alpha < \Phi < \alpha$, with α which can not be neglected (case of contact inside bearings), the above mentioned geometrical relation presents important differences in comparison with Hertz's displacement equation for the contact between two cylinders with parallel axes:

$$w_1 + w_2 = \delta - \frac{1}{2} \left(\frac{1}{R_1} + \frac{1}{R_2} \right) x^2 \quad (5)$$

For this contact case, the contact patch is a rectangle with the width $2b$. The real problem (a reversed problem) was to find a state of pressure which conduces to a radial relative displacement $(\bar{u}_{r2} - \bar{u}_{r1})$ as in relation (4). The problem was solved by Persson [1] who proposed special pressure dependences and functions. Persson's pressure distribution is presented in Fig.3. It may be observed that the contact pressure increase when decreasing the Φ contact angle and when, of course, the sizes of the contact patch decrease too.

The variation of the contact angle limits (the arc) α (for the case $\Delta R > 0$ as well for the case $\Delta R < 0$) function of the normal surface loading Q is presented in Fig.4. In order to obtain a suggestive comparison, the variation proposed by Hertz and Steuermann are plotted on the same system of axes.

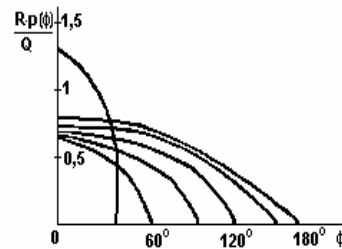


Fig.3. The Persson's contact pressure distribution

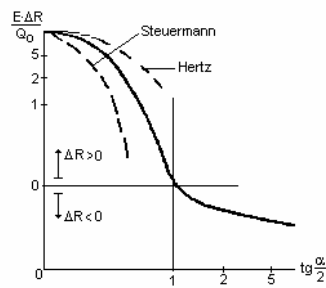


Fig.4. The variation of the contact angle limits (the arc) α function of the normal surface loading Q

It may be observed that the obtained results, according to the above mentioned contact theories, are in agreement only for small values of the normal load Q or for high values of the curvature radius difference ΔR . For high values of the normal load Q or for small values of the curvature radius difference ΔR , the results are far from that obtained with the most accurate Steuermann's theory which consider the bodies in contact as elastic half-spaces.

For the particular case when the two cylinders are manufactured from the same material, E. Pantou proposed the following approximate formula:

$$Q(\varphi) = \frac{Q}{R_1(\sin \varphi_0 \cos \varphi_0 + \varphi_0)} \cos \varphi \quad (6)$$

A similar problem, namely the contact without friction between a sphere and a spherical cavity has been studied by Goodman and Kerr [4]. They concluded that the displacement of the centers of the bodies in contact δ is 25% higher than the displacement predicted by Hertz's theory.

III. PROBLEM SOLUTION

The purpose of the *experimental research* by *photoelasticity* about the state of stress in the component wires of a wire rope consist in the estimation of the percentage deviations of the contact stress calculated values according with Hertz's, Pantou's and Steuermann's theories in comparison with the real values of the stresses. This type of experimental research would ease the choice of the best relation depending on the size of the contact angle φ_0 . In terms of contact problems, the location of the maximum tangential stresses is associated with the initiation and propagation points of several cracks, which require the accurately determining of the stress spectrum in the immediate vicinity of the contact area.

In view of the photoelastic analysis [2] were made two discs having the diameters of 15 and 20 mm and concave surfaces with beams of 26; 20,1 and 15,15 mm. They were made out of optical active and translucent materials. For the achieving of the isochrones photos an installation with two polaroids was used. The polaroids consisted of \varnothing 150 mm of monochromatic light produced by a bulb with downloads of sodium vapors. This installation is part of the endowment of The Laboratory of Strength of Materials from the Mechanical Engineering Faculty belonging to Polytechnic University of Timisoara (Fig.5).

A specimen was made for the calibration of the photoelastic material. This specimen was tested during a pure bending thus determining the photoelastic constant of the material $\sigma_0 = 2,65$ MPa, with a 6 mm thickness. During the tests the goal was not to induce contact requests which could lead to plastically strains. The tests ensured the reproductively of the results, reproductively checked by the lack of residual stress state in the parts after the download, a fact easy found in polarized light.



Fig. 5. The isochrones photos for $R_1/R_2 = 0,58$ at $q = 74,21$ N/mm, the higher level of isochrone $n=8$

The Fig.6 diagram represents the deviation variation of results from the experimental ones depending on the contact angle φ_0 for the two contacts $R_1/R_2 = 0,58$ and $R_1/R_2 = 0,75$ where Hertz's hypothesis is not valid.

From this representation results the fact that the values σ_{ech} calculated after Pantou and Steuermann are grouped in an area of deviation of (+10%...-5%), while when using Hertz's formulas they leads to deviations of approximately (+15%) at $\varphi_0 = 33^\circ$ up to approximately (+40%) at $\varphi_0 = 60,5^\circ$.

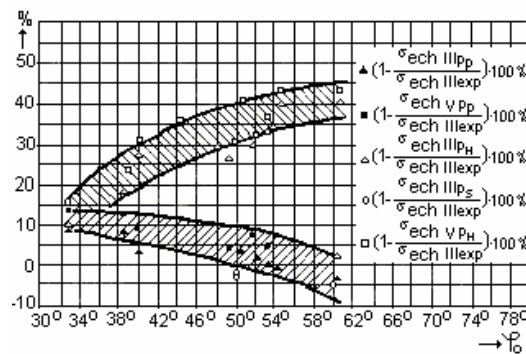


Fig.6. The deviation variation of results from the experimental ones depending on the contact angle φ_0

This percentage error of the results decreases with the rising of the application and with the rising of the maximum order of the isochrones, up to a stresses value of approximately 10 MPa. This leads to an increase due to the value of variation of the elasticity modulus reaching an error of 10% at 20 MPa. This error is introduced by the asymmetry request which couldn't be completely eradicated. The error is compensated by the average

between the readings of the isochrone's order from the two edges of the contact area.

The fatigue alternant loading is the main reason of the degradation of the wire ropes. The results of the compression contact fatigue tests [2], performed on the Nădășan-Boleanțu testing machine placed in the Laboratory of Strength of Materials from the Mechanical Engineering Faculty of Timisoara, are plotted in a diagram (Fig.7) which expresses the dependence between the life-time of a wire with a 1 mm diameter versus the compression contact stress.

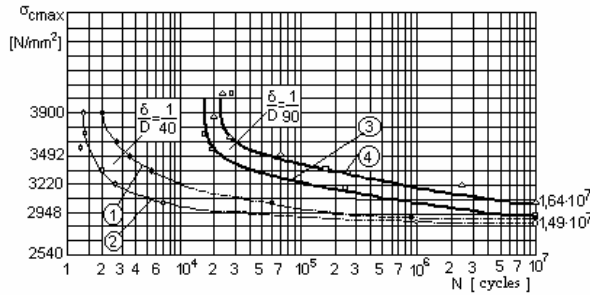


Fig.7. The results of wires fatigue testing on NB machine

A statistical analysis according to the log-normal distribution law has been performed [9]. The value of the life-time of the wires belonging to a traction wire rope obtained after the linearization of the distribution curve, accepting a normal distribution of life-time, is in a perfect agreement with the life-times indicated in the special references when the wire rope considered as an element with a restricted life-time because of the typical working conditions.

The finite element numerical analysis about the local compression effect is the solution for the contact problem between two wires with different or same diameters in contact. Also the contact problem between an external and an internal cylinder shape bodies (Fig.8) has been analyzed [8] by using a hybrid technique considering the contact without friction for all the cases which have been presented above.

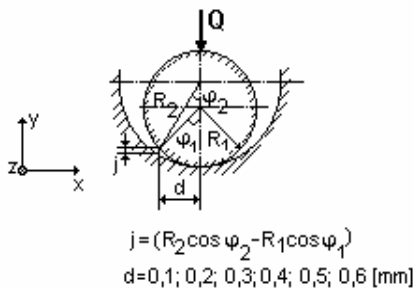


Fig.8. The objective geometry

The induced stress in any point of a normal plane on the contact surface (Fig. 9) is given by:

$$\begin{cases} \sigma_z = -p_0 \frac{1}{\sqrt{1 + \left(\frac{z}{b}\right)^2}} \\ \sigma_y = -p_0 \left[\frac{1 + 2\left(\frac{z}{b}\right)^2}{1 + \left(\frac{z}{b}\right)^2} - 2\frac{z}{b} \right] \\ \sigma_x = -p_0 \cdot 2v \left[\sqrt{1 + \left(\frac{z}{b}\right)^2} - \frac{z}{b} \right] \end{cases} \quad (7)$$

For $z = 0$, which means the points on the centre line of the contact surface, the relation (7) became:

$$\sigma_x = -2vp_0; \quad \sigma_y = -p_0; \quad \sigma_z = -p_0 \quad (8)$$

The maximum shearing stress takes values between zeros to the maximum value:

$$\tau_{\max} = \frac{1}{2}(\sigma_z - \sigma_y) \quad (9)$$

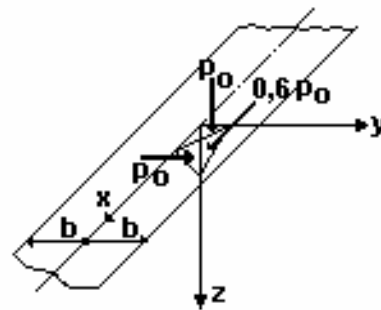


Fig.9. The main normal stress on the points of the centre line of the contact surface

The use of these relations can be done only in the range where the material has an elastic linear behavior [5]. In the case of the steel ropes, it may appear contact stresses between the wires, which can exceed the elastic limit. In this way, there was necessary to perform a study which allows the complex approach of the stress-strain state in all the stress stages. The finite element analysis allows investigating the state of stress both in the elastic and plastic range [10]. Besides, the finite element analysis allows a complex study about the state of stress at the contact between the component wires of a steel rope taking into account the simultaneous reciprocal interactions [6], [7].

In order to simulate the contact between the wires, there have been used GAP finite elements. The GAP elements are defined by two nodes and by the direction given by their connection. The real constant associated with these finite elements represents the maximum relative displacement between those two nodes [5].

There was simulated a contact between two cylinders with the diameter of $d = 1,25 \text{ mm}$. Because of the vertical loading and geometrical symmetry, as well because of the absence of the axial loading, the contact problem has been

investigated in a transversal cross-section of the wire. The calculus model and the meshing [9] in order to perform the numerical analysis of the contact between two parallel similar are presented in Fig.10.

The circular cross-section wires have been meshed by quadrilateral finite elements for a plane state of deformation [7]. In the central core of the wires the state of stresses and deformations can be neglected. The boundary conditions consist in breaking the horizontal displacements of the finite elements located in the opposite side of the contact patch. Then the loading is simulated by a uniformly distributed pressure. The calculus model incorporates also two finite elements TRUSS 2D (beam elements with joints on the ends) in order not to allow the displacements both in horizontal and vertical directions [10].

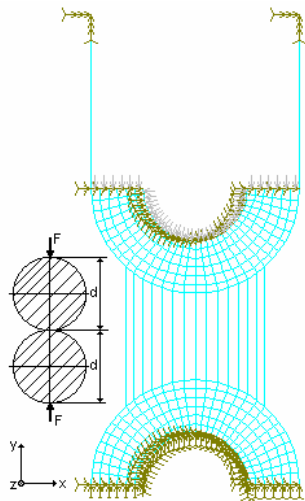


Fig.10. The calculation algorithm for the contact of two wires a 1,25 mm diameter

As a result of the finite element analysis [9], the components of the stress and deformation tensors have been post-processed for the simulated contact. Taking into account the maximum and minimum values of the tensors' components, there have been used 9 stages for an equal representation (Fig.11).

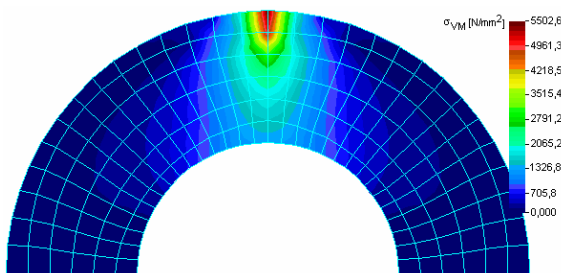


Fig.11. The equivalent von Mises stress σ_{VM} [N/mm²], the case of loading $Q = 73,7$ N

The contact between the central core-wire and the adjacent wires of a steel rope has been simulated [9] by the contact between cylinders with parallel axes. As a consequence of the geometrical and of the loading symmetry there has been considered the contact case

between a central core-wire and three adjacent wires, as in Fig.12.

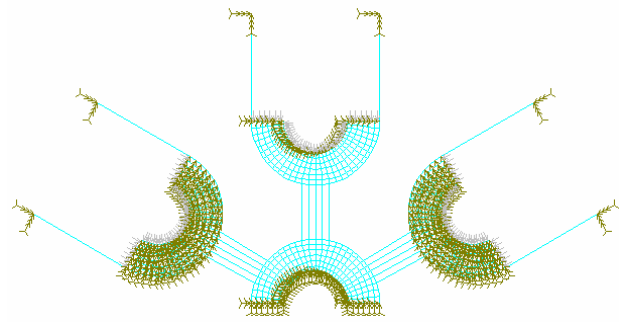


Fig.12. The calculation algorithm for the contact of wire rope strands (751 elements; 874 nodes)

The results of the finite element analysis are post-processed as strips of equal stress and equal displacement. There can be observed in Fig.13, that the state of stress in a wire has no influence about the state of stress in the adjacent wires in contact, even there is a theoretical symmetry of stresses and deformations in the twisted wires [1].

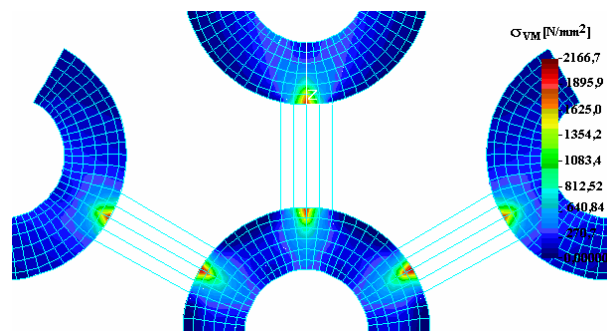


Fig.13. The equivalent von Mises stress σ_{VM} [N/mm²], case of loading $Q = 73,7$ N

There was simulated [9] a contact between a cylinder with the radius $R_1 = 0,625$ mm and a cylindrical cavity with the radius $R_2 = 0,6313$ mm ($R_1/R_2 = 0,99$). From a physical point of view, the differences in diameter between the surfaces in contact are little.

Because the maximum stress develops around the contact area, the calculation algorithm that was used (Fig.14) shows a change in the geometry of the contact surface. This is possible because of the association for the finite contact elements, as objective constants of objective distances calculated by taking into consideration the objective geometry (Fig.8).

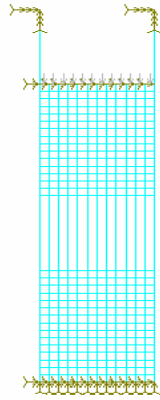


Fig.14. The calculation algorithm for the contact between a cylinder and a cylindrical cavity

In Fig.14 there have been presented the calculation model where the cylindrical shape is simulated by the presence of the gap elements between those two bodies. For this calculation model there were running 6 loading cases. The loading cases represent different steps of loading between the minimum and the maximum value of the force Q (Fig.8).

The calculation algorithm contains 651 plain finite 2D elements of rectangular shape for the plain state of deformation and 416 nodes. The boundary conditions stop the horizontal movement of the elements from the opposite area of contact, which are then loaded with normal charge, uniformly distributed per unit of length for simulating the contact between two bodies. The calculation algorithm also includes the two finite TRUSS 2D elements, bar-type of low-rigidity elements, which joints at the ends in order to stop the horizontal and vertical movement.

After the running on of the software, all the components of stress and deformation tensors have been performed for 9 equal representation steps in function of the maximum and the minimum variation limits of stresses and deformations (Fig.15). Results are presented as special tables and diagrams about the stress and deformation fields. It can be observed that the state of stress and deformation is similar for every two adjacent wires in contact.

The non-linear analysis performed has permitted a complete study of the stress-strain state at the contact surfaces level. For each step there have been calculated the forces which appear in the gap elements. The evolution in time of the forces from the gap elements shows the dimensions and the changes, which appear for the contact surface between the interacting bodies.

The results are visualized in equal stress bands in Fig.15, respectively in equal moments bands in Fig.16.

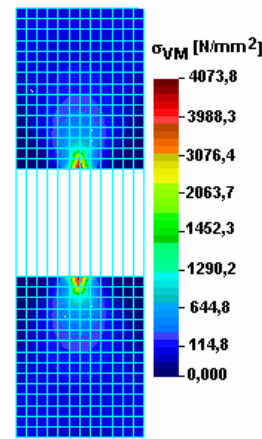


Fig. 15. The equivalent von Mises stress σ_{VM} [N/mm²] for the considered stress model, case of loading $Q = 45$ N

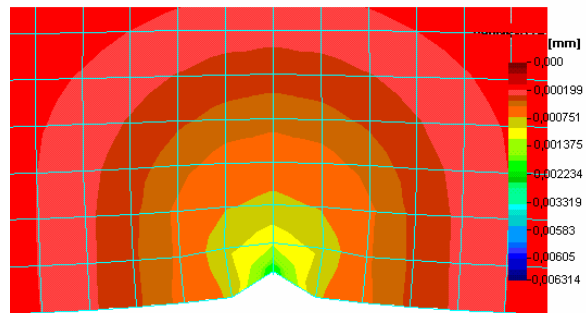


Fig.16. The resultant displacements [mm] for the cylinder of radius $R_1 = 0,625$ mm, case of loading $Q = 21$ N

The results are graphically processing (Fig.17) and will be used to calculate the fatigue crack propagation and to estimate the steel rope working life.

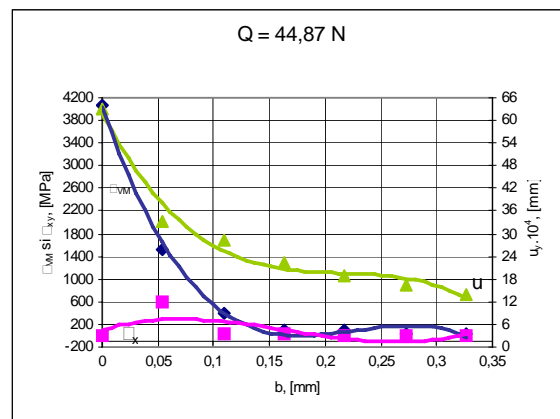


Fig.17. The variation of σ_{VM} ; τ_{xy} [N/mm²] and the vertical displacement on the half-breadth of the contact surface, case of loading $Q = 45$ N

The analysis about the life-time of the component wires of a steel wire rope by finite element numerical analysis presents the opportunities to use dedicated software [8], which is typical for the analysis of the behavior of wires under variable loading as well for the life-time estimation.

The contact between two wires with the same diameter of 1,25 mm loaded with a pressing force of (3,6...327,5) N has been analyzed [9].

The finite element numerical analysis of the degradation of the wires because of an alternant loading has been performed for the contact between two wires with same diameters of 1,25 mm, for 9 loading cases. The fatigue phenomenon because of the maximum σ_y stresses which are perpendicular on the contact area has been analyzed after the loading fatigue block (Fig.18) has been imposed ($\sigma_{y_{max}}$ - in function of the number of cycles).

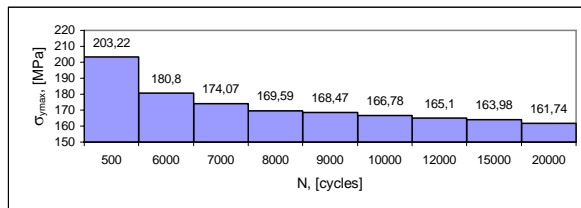


Fig.18. Loading fatigue block $\sigma_{y_{max}} - N$

During this program the fatigue limit curve (Fig.7 - curve 1) for an alternative-symmetrical loading cycle of a non-torsion wire, bent on a segment lacking a channel and with the diameter of 40 mm, was used.

The stages to be followed to introduce the data and to use the software [10] are:

- 1) – The running of the Finite Element software for the contact between two wires with equal diameters of 1,25 mm, for the testing cases.
- 2) – The 9 testing loading steps and the associated number of cycles are entered.
- 3) – The central surface contact node (where the maximum stress $\sigma_{y_{max}}$ is present) is prescribed.
- 4) – The fatigue limit curve (7 points on the curve 1, Fig.6) is introduced. The curve followed an alternative-symmetrical loading cycle with a non-symmetry coefficient of $R_s = -1$.
- 5) – The prescription for the results calculation is accurately defined.
- 6) – The software is running on according to the orders Analysis > Fatigue > Run Fatigue Analysis.

The present calculus connects the stresses in wires, caused by the compression contact; with the lifetime of the traction wire ropes subjected to particular variable loading which have a specific nature for the working on of wire ropes.

After the software running on, the cumulative deterioration coefficients for every loading steps and the total cumulative deterioration coefficient have been obtained. The value of the total cumulative deterioration coefficient was of 6,75. A similar procedure has to be used in order to estimate the cumulative deterioration coefficient for any real loading cycle.

IV. CONCLUSION

* A comparison between the results obtained by Steuermann and Hertz (Fig.19) leads to the following conclusion: when the ratio $\frac{q}{E(R_2 - R_1)}$ increase, the

difference between the results (according to the above mentioned theories) also increases. Anyway, there is a relative good agreement between the results for contact angles less than 20° .

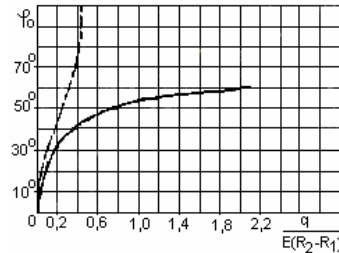


Fig.19. Comparison between Steuermann's and Hertz's results

* There is presented in Fig.20 the distribution $Q(\varphi)$ for three values of the contact angle: $\varphi_0 = 30^\circ, 50^\circ$ and 60° according to Pantón's (non-continuous line) and Steuermann's theories (continuous line). It may be observed in Fig.20 that the results according to the above mentioned two theories are in a perfect agreement when increasing the contact angle φ_0 .

* The most important conclusion is that for a significant contact patch, the contact problem between a cylinder and a cylinder cavity may be solved only by Steuermann's theory instead of it's mathematical sophisticated apparatus.

* In comparison with the contact of same diameter wires (Fig.11) when the maximum stress σ_{VM} reach the value of 5502,8 [N/mm²] because of a 3D state of stress in case of wire-ropes, there is a compensation effect which reduce about 3 times the level of maximum stress σ_{VM} (Fig.13) which reach the value of 2166,7 [N/mm²]. In the same manner, the absolute displacements are 3 times less for the contact between the central core and the adjacent strands in comparison with the absolute displacements for the contact between two parallel and identical wires.

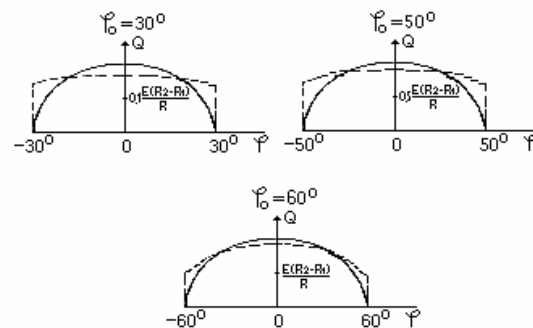


Fig.20. The distribution $Q(\varphi)$ according to Pantón's (non-continuous line) and Steuermann's theories (continuous line)

From the analysis of the graphical processing of the results about the contact between a cylinder and a cylindrical cavity we can reach the following conclusions:

* The equivalent von Mises stress σ_{VM} [N/mm^2] has a maximum value in the center of the contact surface, decreasing to its extremities.

* The tangential stress τ_{xy} [N/mm^2] is zero in the center of the contact surface, where the triaxial compression appears [1]. The maximum value of the tangential stress corresponds to the value of the half-breadth of the contact surface $b = 0,0545$ mm, decreasing to its extremities.

* The vertical movement is greatest possible in the middle of the contact surface, situation that can be visualized by representing the deforming state by bands of equal movement on the deformed position of the cylinder (Fig.16).

REFERENCES

- [1] T. Babeu, *The Basic Theory for Resistance of Materials*, Mirton Publishing House, Timisoara, 1998.
- [2] L. BoleaŃu, *Studies about the strength of traction wire ropes and wires*, Ph.D. dissertation, Lito.IPT, 1968, Timisoara.
- [3] N. Faur, I. Dumitru, *Finite differences and finite elements in resistance of materials*, Mirton Publishing House, Timisoara, 1997.
- [4] E. Ghita, *Resistance and working life at solid bodies'contact*, Mirton Publishing House, Timisoara, 2000.
- [5] T.Y. Yang, *Finite Element Structural Analysis*, Prentice-Hall, 1986.
- [6] Z. Kala, J. Kala, Variance-Based Sensitivity Analysis of Stability Problems of Steel Structures Using Shell Finite Elements and Nonlinear Computation Methods, *In Proceedings of the 2nd WSEAS International Conference on Engineering Mechanics, Structures and Engineering Geology (EMESEG'09)*, Rhodes Island, Greece, 2009, pp.89-94.
- [7] A. Omishore, Advanced Modeling Approached for Reliability Analysis of Steel Structures, *In Proceedings of the 3rd WSEAS International Conference on Engineering Mechanics, Structures and Engineering Geology (EMESEG'10)*, Corfu Island, Greece, 2010, pp.172-176.
- [8] D. Simian, Advanced Computational Techniques, Algorithms and Numerical Methods for Modeling, Simulation and Optimization, *In Proceedings of the 4th WSEAS International Conference on Engineering Mechanics, Structures and Engineering Geology (EMESEG'11)*, Corfu Island, Greece, 2011, pp.17-23.
- [9] L. Vilceanu, *Resistance and working life at steel wire ropes in contact*, Mirton Publishing House, Timisoara, 2003.
- [10] O.C. Zienkiewicz, R. L. Taylor, *La method des elements finis*, AFNOR Paris, 1991.